

# Characterization of PM<sub>2.5</sub> by X-ray diffraction and scanning electron microscopy–energy dispersive spectrometer: its relation with different pollution sources

P. G. Satsangi · S. Yadav

Received: 30 November 2011 / Revised: 5 November 2012 / Accepted: 25 December 2012 / Published online: 28 February 2013  
© Islamic Azad University (IAU) 2013

**Abstract** Atmospheric PM<sub>2.5</sub> samples were collected by using Mini-Vol TAS air sampler. Samples were characterized directly on the collecting substrate using X-ray diffraction and scanning electron microscopy–energy dispersive spectrometer. From the analysis, it was found that Si dominate over other elements which follows the trend as Si > S > Zn > Cu > Na > Al > K > Ca > P > Fe > Mg > Ti. Based on the measurements of a population of 840 particles, particle morphology was determined by quantitative image analyzer and value of roundness (*R*) varies from 0.23 to 1.0 (mean 0.75) which suggests that particles vary in shape from nearly irregular to perfectly spherical shape. The mineral particulate matter identified in the atmosphere of Pune was made up of: silicates (52 %), oxides (22 %), sulfates (8 %), phosphates (7 %), carbonates (3 %) and others. A factorial analysis was carried out to determine the main elements related to the emission sources such as soil and building material erosion (~44.6 %); oil combustion (20.6 %) and fuel and biomass burning (18.3 %). Besides these factors, soot particles are abundantly present in all studied samples. Mineral particles such as sulfates aggregated to soot could have produced localized climatic effect in Pune. The emphasis of the present study is to give insight and detailed analysis of morphological and chemical composition of atmospheric particles at discrete level.

**Keywords** Elemental composition · Minerals · Particulate morphology · Soot

## Introduction

Particulate matter (PM) suspended in the atmosphere comprises a complex mixture of different elements and compounds. A series of epidemiological studies have shown a clear association between effects on health and environmental concentrations of PM (Dockery et al. 1993; Wilson and Suh 1997; Kunzly et al. 2000) especially its “fine” component ( $\leq 2.5 \mu\text{m}$  (PM<sub>2.5</sub>) (Schwartz et al. 1996). The sources, characteristics and potential health effects of the larger or coarse particles ( $> 2.5 \mu\text{m}$  in diameter) and smaller or fine particles ( $< 2.5 \mu\text{m}$  in diameter) are different; the latter can more readily penetrate into the lungs and are therefore more likely to increase respiratory and mutagenic diseases (Schwartz et al. 1996). A typical PM contains various components: sulfate (mostly ammonium and calcium), nitrates (mostly ammonium), chlorides (mostly sodium), elemental and organic carbon (especially traffic-related soot), biological materials, iron compounds, trace metals, and minerals derived from rocks, soils and construction.

India being a tropical country, the PM loading is higher as compared to other latitude and soil is its major contributor. Besides natural, industrial and vehicular emissions contribute most pollution problem in urban area of India. Data concerning fine and ultrafine particulate in urban area show that the atmospheric concentration of these particulate fractions can be estimated at  $10^4$  and  $10^5$  particles/cm<sup>3</sup> and can greatly exceed such value during heavy traffic (Zhu et al. 2002). The large surface areas provided by tiny average-size airborne minerals result in abundant crystallographic sites for heterogeneous condensation and subsequent reactions of gaseous species (Dentener et al. 1996; Zhang and Carmichael 1999). They are important as absorber and scatterer of radiation and may have important

P. G. Satsangi (✉) · S. Yadav  
Department of Chemistry, University of Pune,  
Pune 411 007, India  
e-mail: pgsatsangi@chem.unipune.ac.in

effects on climate (Andreae 1995; Duce 1995; Li et al. 1996), especially on local and regional scale because of their relatively localized spatial and temporal distribution. However, some minerals (like soot) will produce warming effect and thus could be considered as ‘greenhouse particles’, whereas others will produce negative forcing (like sulfate) and thus tend towards cooling considered as ‘ice-house particles’ (Buseck et al. 2000). They may also represent a danger for animal and vegetal life and have important consequences for visibility (Jung and Kim 2006) and take part in the darkening and damage of historical buildings or in climate change (Rodriguez et al. 2009).

In general, the abundant group of particles by mass (~50 %) globally consists of mineral and their study and environmental impacts have been relatively overlooked. The assessment of pollutants, identification of their sources and transportation is a prerequisite for understanding their effects on human health as well as on climate. In view of establishing their origin and their potential effects on human health and on the climate, elemental composition of individual aerosol particles is sometimes more useful than their bulk elemental composition. The morphology of atmospheric particles received significant importance in recent years due to effect of the particle shape on their radiative (as climate effect) (Adachi et al. 2010) and chemical properties (as health effect) (Ghio and Devlin 2001). To determine the elemental composition, size and shape of PM, scanning electron microscopy (SEM) combined with energy dispersive spectrometer (EDS) provides all these information. Thus, it is a useful technique in distinguishing particles originating from different sources based on their chemical composition and morphological characteristics. The studies on elemental composition of atmospheric particles are rather limited (Querol et al. 1999, 2002; Pina et al. 2000, 2002; Shi et al. 2003; Breed et al. 2002; Ekosse et al. 2004; Mathis et al. 2004; Suzuki 2006). SEM–EDS has been used by researchers for identification of particulate morphology and elemental composition (Chabas and Lefevre 2000; Ma et al. 2001; Liu et al. 2005; Li et al. 2011). In Indian context, very few comprehensive studies using SEM–EDS have been done (Cong et al. 2010; Sharma and Srinivas 2009; Srivastava et al. 2009; Pipal et al. 2011) and in Pune region this type of study has not been reported so far. Present study was carried out for two consecutive years of 2010 and 2011 from June to September keeping the following objectives: (1) to investigate the mineralogy identification by X-ray diffraction (XRD) of the PM<sub>2.5</sub> of Pune city; (2) morphology (by SEM–EDS) of the particles and (3) to identify the possible sources and origin based on the chemical composition of the PM<sub>2.5</sub>, as different kinds of mineral particles may act not only additively but also in a synergistic way in their health effects. Moreover, the obtained information from XRD and

SEM–EDS is preliminary but still it will be useful for understanding the air quality of city in terms of health and climate purpose.

## Materials and methods

### Site description

Pune (18° 32'N, 73° 51'E) is located 560 m (1,840 ft) above sea level on the western margin of the Deccan plateau. It is situated on the leeward side of the Sahyadri mountain range, which form a barrier between the Arabian Sea. City is surrounded by hills and mountains. Just outside the city, Sinhagad fort is located at an altitude of 1,300 m. Pune has a tropical wet and dry climate with average temperatures ranging between 20 and 33 °C. The monsoon lasts from June to October, with good rainfall and temperatures ranging from 10 to 28 °C. In the city, most of the annual rainfall of ~722 mm (28.4 inches) falls between June and September, and July is the wettest month of the year. Today, Pune has a diverse industrial population. It is one of India's most important automotive hubs, with some domestic and international auto giants manufacturing units. Pune also has hundreds of large and small IT companies. Pune has well-established glass, sugar, and forging industries. Pune is the rapidly growing city in terms of industrial installations, vehicular population and also urbanization due to the boom in housing industry, since last few years. As per the 2010 Census of India estimate, the population of the Pune urban agglomeration is to be around 5,518,688. The population of the urban agglomeration was estimated to be around 4,485,000 in 2005. The migrating population rose from 43,900 in 2001 to 88,200 in 2005.

The sampling site considered for this study is Department of Chemistry, University of Pune. University of Pune is surrounded by variety of deciduous trees. No industries are located in the vicinity of the sampling sites. Major traffic junction (i.e., University circle) and a railway line are nearly 1 and 3 km from the sampling site. The principal sources of contamination are traffic, biomass burning and construction activities in and around the vicinity of sampling site.

### Sampling and analysis

#### Sample collection

Sampling of PM<sub>2.5</sub> was carried out at a height of 12 m from the ground level at terrace of Department of Chemistry, University of Pune, Pune, between June and September for two consecutive years (i.e., 2010 and 2011) (Fig. 1). 24-h PM<sub>2.5</sub> samples were collected with (Mini-Vol TAS air

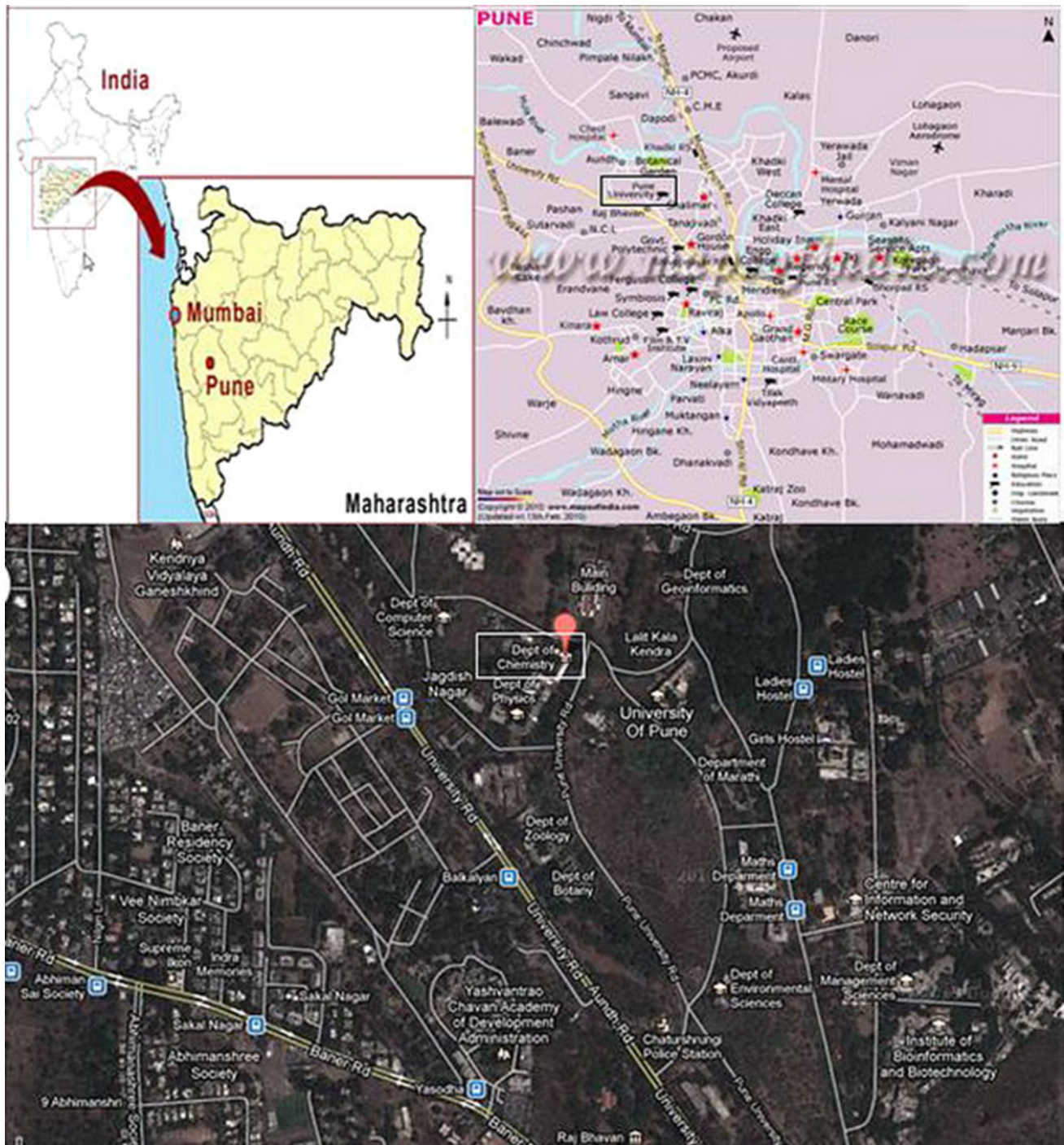


**Fig. 1** Map showing the sampling site

sampler) particulate sampler which runs at a constant flow rate of 5 LPM. The particles ( $PM_{2.5}$ ) were collected on 47-mm diameter PTFE filter papers. PTFE filter has a fiber structure and good for studying the gravimetric as well as elemental analysis by XRD. For morphology study, PTFE filter is causing the positive artifacts and uncertainties because of its fiber structure. But, still some studies have

been reported SEM–EDS on PTFE (Wheeler et al. 2000; Xie et al. 2009; Slezakova et al. 2008; Pipal et al. 2011). Moreover, present study was performed during the monsoon season (June–September) when the relative humidity is very high (80–90 %). In this regard, PTFE is very stable and absorbing negligible water or gases. It has inherently low contamination levels.

### Gravimetric analysis

PM masses were determined gravimetrically by subtracting the initial average mass of the blank filter from the final average mass of sampled filter. Filters were repeatedly weighed (Shimadzu AUX 220; sensitivity  $\pm 0.1$  mg) until three reproducible values were obtained. Filters were equilibrated in silica gel desiccators for 24 h before weighing, to eliminate the effect of humidity and also to obtain accurate PM measurements. Field blank filters were also collected to reduce gravimetric bias due to filter handling during and after sampling. Filters were handled with Teflon tape-coated tweezers to reduce the possibility of contamination. It is assumed that the particulate deposited on filter papers were uniformly distributed over entire area.

### Sample analysis

#### Scanning electron microscopy (SEM)

Scanning electron microscopy coupled with energy dispersive X-ray analysis (EDS) (JEOL JSM-6330F, JEOL Ltd., Akishima, Tokyo, Japan) was used for characterization, viz. morphology (shape and size) and chemistry of airborne particles. SEM is high-resolution surface imaging method which uses an electron beam. The samples (dry filter papers) were randomly cut in  $1\text{ cm}^2$  size out of the main filter. A very thin film of platinum (Pt) was deposited on the surface of the samples to make them electrically conductive. These samples were mounted on electron microprobe stubs. The SEM–EDS analyses were carried out with the help of a computer controlled field emission SEM equipped with EDS detection system at the Department of Physics, University of Pune. In the present investigation, the SEM was used in its most common mode i.e., emissive mode. The other parameters are as follows, Detector: Si (Li), Limit of detection, 500,000; accuracy, 10 %; energy, 20 kV (accelerating voltages, 0.5–30 kV). Elements with atomic number less than 6 were not determined. Carbon and fluorine were also not considered in present discussion due to their presence on the filter substrate.

#### X-ray diffraction (XRD)

The identification of the crystalline PM of the samples was performed using X-ray powder diffraction with a Bruker, D8-Advance and X-ray diffractometer with Cu-K $\alpha$  radiation (40 kV and 40 mA), from  $3^\circ$  to  $50^\circ$ , at a rate of  $3^\circ$  (2 $\theta$ )/min, and the sampling distance was  $0.01^\circ$  (2 $\theta$ ). The filters with PM<sub>2.5</sub> samples were cut into  $1\text{ cm}^2$  pieces and placed on aluminum sample holder for XRD qualitative analysis. The

XRD analysis was performed in the Department of Physics, University of Pune. Each mineral has its own chemical composition and special crystal structure, which can be identified by ensuring 'd' value given in XRD-JCPDS (Committee on powder diffraction standards).

#### Image analysis

Particle morphology was determined by quantitative image analyzer (IA) using Image-J software. SEM micrograph was digitized, image processed and primary feature data measurements were made; including count, area ( $A$  the total number of detected pixel within the feature), length ( $L$  length of longest feret), breadth ( $B$  length of shortest feret) and perimeter ( $P$  the total length of the boundary of the feature). These data measurements were automatically obtained using the software. All dimensional parameters were measured in calibrated units (microns). Particle size distribution of all parameters was calculated using SPSS (Version-16). Parameters derived from the primary feature measurements include aspect ratio (AR ratio of  $L/B$ ), and roundness ( $R$ , a shape factor which gives a minimum value of unity for a circle.  $R$  is calculated through the following equation (Eq. 1);

$$R = (\text{Perimeter})^2 / 4\pi \text{ area} \quad (1)$$

In addition, estimations were also made of equivalent spherical diameter (ESD), a commonly used parameter for particle sizing using following equation (Eq. 2)

$$\text{ESD} = 2 \sqrt{\frac{\text{Area}}{\pi}} \quad (2)$$

(QUARG 1996; Berube et al. 2004). Both particle surface area ( $SA$ ,  $\mu\text{m}^2$ ), and volume ( $\mu\text{m}^3$ ) can be derived by following equations (Eq. 3 and Eq. 4);

$$SA = 4\pi \times [(\text{ESD})/2]^2 \quad (3)$$

$$V = 4/3 \times \pi \times [(\text{ESD})/2]^3 \quad (4)$$

### Results and discussion

The average mass concentration of PM<sub>2.5</sub> at Pune was found to be  $46.2 \pm 2.3\ \mu\text{g m}^{-3}$ . The observed concentration is 1.6 times higher than the WHO standards ( $25\ \mu\text{g m}^{-3}$ ) and slightly higher than the NAAQS ( $40\ \mu\text{g m}^{-3}$ ). Table 1 depicts the average weight percentage of all the elements determined by SEM–EDS. As depicted from the table, oxygen-rich particles dominate over other elements which follows the trend as  $\text{Si} > \text{S} > \text{Zn} > \text{Cu} > \text{Na} > \text{Al} > \text{K} > \text{P} > \text{Fe} > \text{Mg} > \text{Ti}$ . Based on the measurement of a population of 840 individual particles, the physical characteristics of particles are also

**Table 1** Morphological and elemental characteristics of deposited particles in study area

Count:840	Mean	SD	Min.	Max	Sum
<b>Morphological characteristics</b>					
A ( $\mu\text{m}^2$ )	1.12	1.05	0.03	9.17	NA
L ( $\mu\text{m}$ )	1.35	0.92	0.28	4.63	NA
B ( $\mu\text{m}$ )	0.92	0.55	0.16	3.23	NA
P ( $\mu\text{m}$ )	3.73	2.49	0.68	13.30	NA
AR	1.10	0.36	1.00	4.00	NA
R	0.75	0.16	0.23	1.00	NA
ESD ( $\mu\text{m}$ )	0.97	0.34	0.20	3.4	NA
SA ( $\mu\text{m}^2$ )	3.97	1.4	0.13	36.0	957
V ( $\mu\text{m}^3$ )	1.29	2.3	$4.3 \times 10^{-3}$	20.6	312
<b>% Contribution of each elements in PM<sub>2.5</sub></b>					
C	48.2	18.8	29.5	75.0	NA
O	14.3	9.3	6.63	31.1	NA
Na	1.68	0.19	0.24	2.13	NA
Al	1.36	0.8	0.41	1.92	NA
Si	3.14	0.32	0.82	4.10	NA
P	0.98	0.10	0.48	1.23	NA
S	2.89	0.23	1.25	3.80	NA
Ti	0.49	0.13	0.14	0.86	NA
Ca	1.24	0.32	0.51	1.49	NA
Mg	0.69	0.52	0.18	0.93	NA
Fe	0.89	0.4	0.28	1.32	NA
Cu	2.12	0.32	1.3	3.89	NA
Zn	2.77	0.48	1.1	4.12	NA
Pb	0.62	0.41	0.32	1.62	NA
As	0.85	0.38	0.21	1.48	NA
K	1.3	0.25	0.28	1.98	NA

summarized in Table 1. Particle morphology parameters, viz. perimeter, area, roundness, ESD and volume, etc., was determined by quantitative image analyzer (ImageJ). As depicted in table, value of roundness (*R*) varies from 0.23 to 1.0 (mean 0.75) which suggests that particles vary in shape from nearly perfectly spherical to irregular shape. ESD varies from 0.20 to 3.4 (mean 0.97) shows that all population are well versed with the aerodynamic cut of the sampler, i.e., PM<sub>2.5</sub>. Both can be clearly viewed from the histogram (Fig. 2a, b) illustrating the distribution of entire data of roundness and ESD of particles. The surface area (SA) and volume (*V*) data include the sum of the values for 840 particles as these are important factors in toxicology assay.

**XRD of deposited particles**

The identification of the mineral in particulate matter (PM<sub>2.5</sub>) was performed using X-ray diffraction. In XRD, major peaks were observed in between 10 and 40 (*2θ*) as

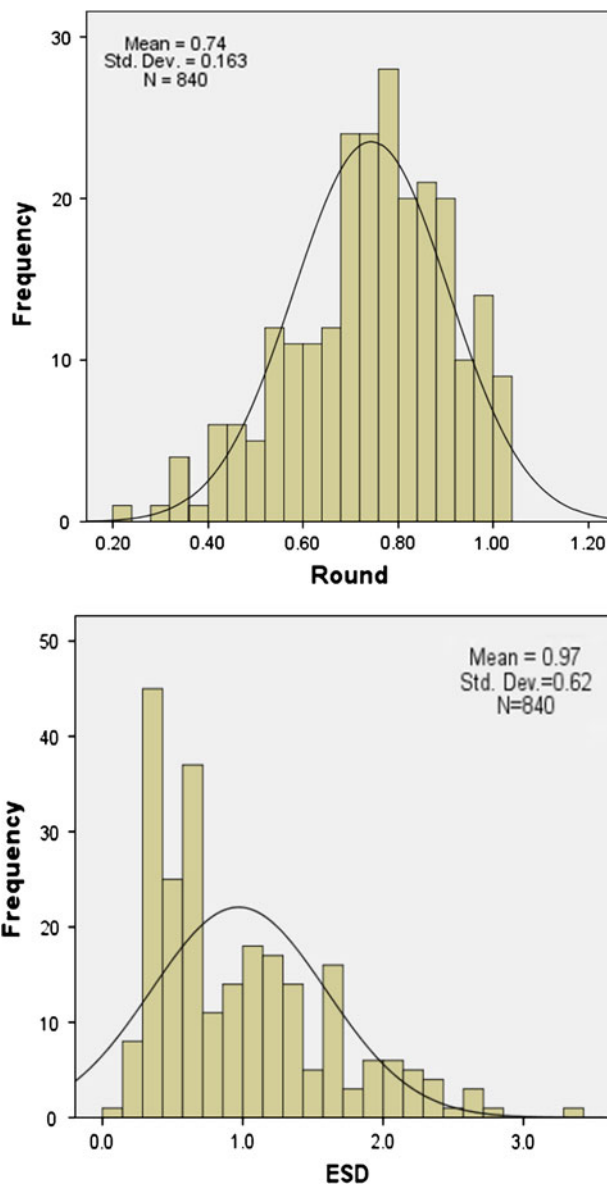


**Fig. 2** Histogram of roundness and ESD of deposited particles

shown in Fig. 3. The mineral PM identified in the atmosphere of Pune is made up of silicates, oxides, sulfates, phosphates, carbonates and others. Figure 4 shows the average proportion of the grouped minerals present in Pune during the study period. Silicates are present as quartz, wollastonite (CaSiO<sub>3</sub>), vermiculite (MgAlFeSiO<sub>7</sub>), kaolinite (AlSi<sub>2</sub>O<sub>5</sub>(OH)) and calcium aluminum silicates; oxides as calcium iron oxide, magnetite and wuestite (FeO); sulfates as gypsum, kocktaite (NH<sub>4</sub>)<sub>2</sub>Ca(SO<sub>4</sub>)<sub>2</sub>, (NH<sub>4</sub>)<sub>2</sub>SO<sub>4</sub>; phosphates as magnesium phosphate (Mg<sub>2</sub>P<sub>2</sub>O<sub>7</sub>) and silicon phosphates (SiP<sub>2</sub>O<sub>7</sub>); carbonate as dolomite (Ca(Mg(CO<sub>3</sub>)<sub>2</sub>); others as iron–zinc (Fe<sub>3</sub>Zn<sub>10</sub>), aenigmatite (Na<sub>2</sub>Fe<sub>5</sub>TiSi<sub>6</sub>O<sub>20</sub>) and halite (NaCl). From the Fig. 4, it can be observed that most of abundant minerals in PM<sub>2.5</sub> in sampling site were silicates (52 %) followed by oxides

(22 %), sulfates (8 %), phosphates (7 %), carbonates (3 %) and others.

### Morphology of deposited particles

Morphology and chemical composition of particle can help to know their sources. Micrographs of the different particles deposited on the filters are shown in Fig. 5 along with their sizes. From Fig. 5a–i, it can be inferred that the particles are rectangle, cubes, capsule, rough rectangle and spherical and an agglomerates types. In general, according to morphology it can be divided in two categories; particles

of natural origin (soil dust or minerals) and anthropogenic origin. Morphology of natural origin are solid and having irregular shapes (Buseck et al. 2000) and mostly dependent on mineral habits, its composition, lifetime and transportation in atmosphere. Particles produced from the combustion processes are both solid and liquid particles with the variable morphologies; in general, particles with spherical shape are the result of the secondary reactions (Li and Shao 2009b) while irregular particles in the fine range result from coagulation processes (Breed et al. 2002). This type of particles occurs as individual particle as well as in aggregated form numerous in the current study.

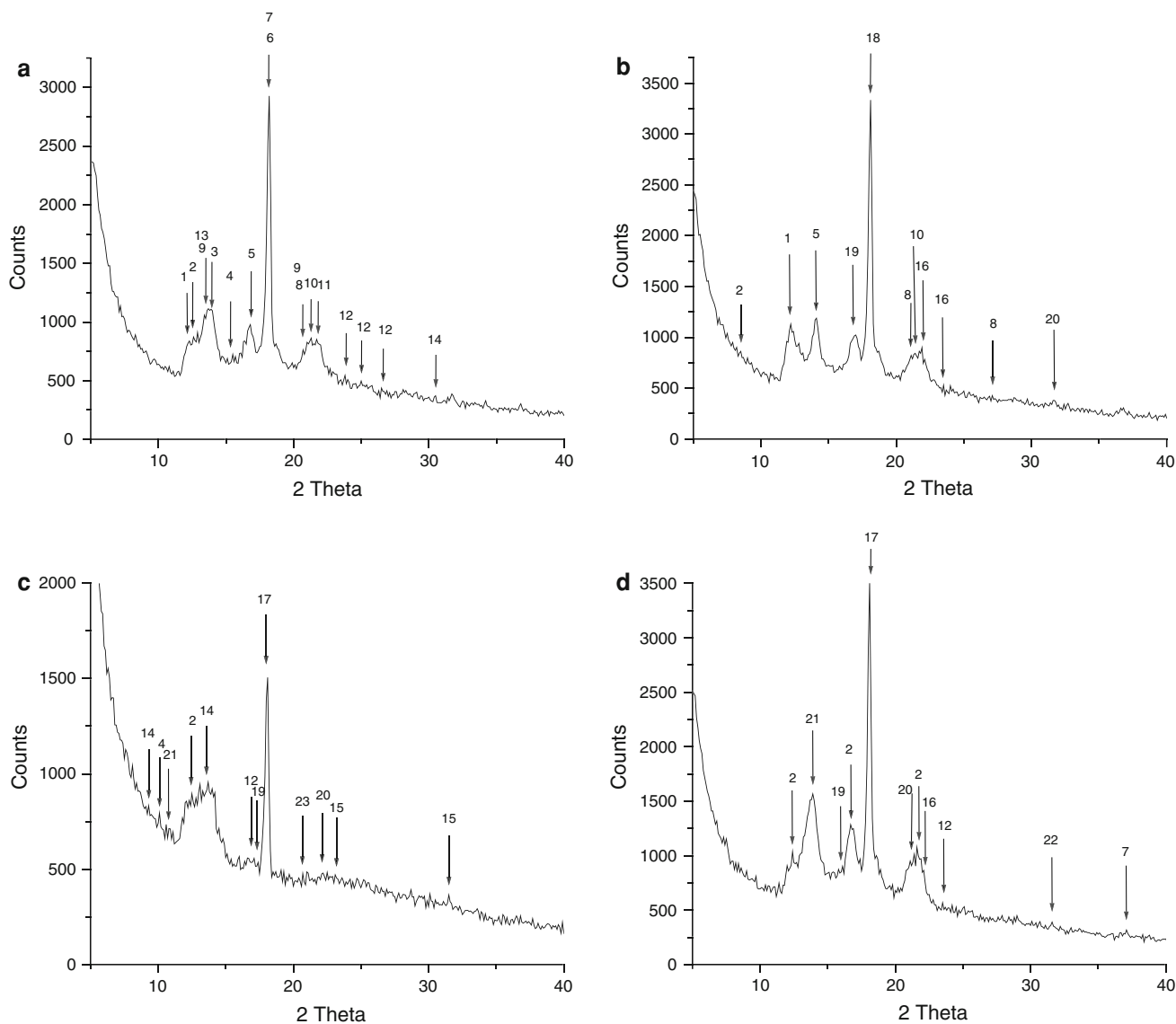
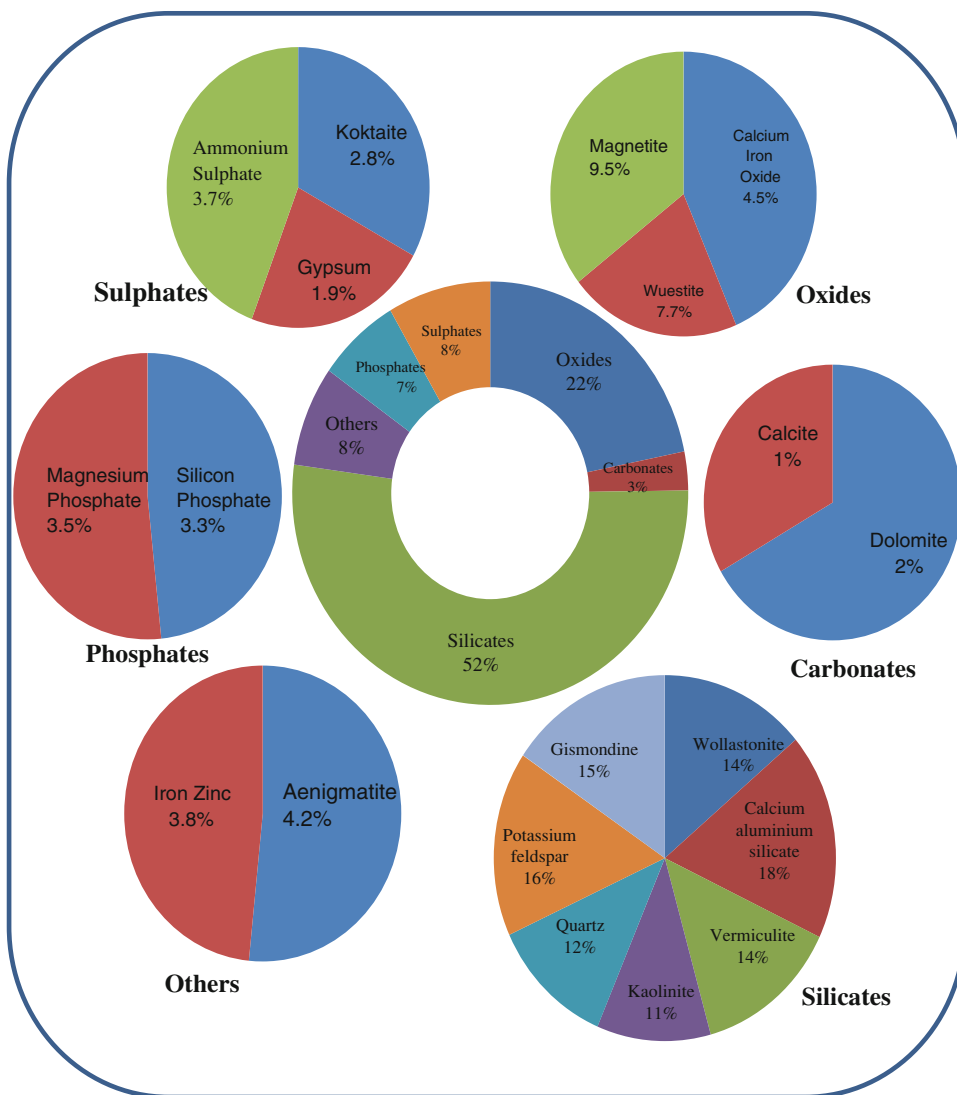


**Fig. 3** X-ray diffraction patterns of PM<sub>2.5</sub> from Pune site. Symbols: 1 Kaolinite (12.3), 2 wallostonite (12.5, 8.5, 21.6), 3 Iron–zinc Fe<sub>3</sub>Zn<sub>10</sub> (13.8), 4 Wuestite (15.4, 10.1), 5 Ammonium sulphate (NH<sub>4</sub>)<sub>2</sub>SO<sub>4</sub> (16.8, 14.1), 6 Dorrite (18.2), 7 Magnetite (18.2, 37.0), 8 Quartz SiO<sub>2</sub> (20.9, 21.2), 9 Magnesium phosphate Mg<sub>2</sub>P<sub>4</sub>O<sub>12</sub> (20.9, 13.7), 10 Silicon phosphate Si(P<sub>2</sub>O<sub>7</sub>) (21.3), 11 Kokaite (21.7), 12 Gypsum

(23.7, 24.01, 27.5), 13 Feldspar (13.7), 14 Calcium aluminium silicate (30.5, 9.3, 13.6), 15 Calcite (31.5), 16 Vermiculite (21.8, 23.5), 17 Calcium iron oxide (18.1), 18 Calcium silicate (18.07), 19 Dolomite (16.9), 20 Magnesium phosphate Mg<sub>2</sub>P<sub>2</sub>O<sub>7</sub> (21.1, 21.4), 21 Aenigmatite (10.9, 13.8), 22 Halite (31.5), 23 Muscovite (20.6). Values in parenthesis indicate 2θ values

**Fig. 4** Average percentage proportion of grouped minerals in Pune



Micrographs also clearly show some irregularly shaped particles. These particles are mixed in composition and are assumed to be the result of chemical reactions between pre-existing particles, liquid or gaseous phase. Li and Shao (2009b) have also suggested that alkaline mineral particles react with gaseous species (such as SO<sub>2</sub>, NO<sub>2</sub> and HNO<sub>3</sub>) and form the coating on the pre-existing particles of minerals.

**Source identification and source apportionment of PM**

A total of 840 data of individual SEM–EDS analyses of particles were statistically analyzed using SPSS (ver. 16) software, with the purpose of determining the correlation and loading factors of particles observed at Pune station.

Correlation coefficient is the measure of the degree of linear relationship between two or more variables. Correlation between elements suggested the likely sources of pollutants and also indicated similar occurrence of element

in the atmosphere. Table 2 shows the correlation coefficient between different elements analyzed by SEM–EDX. Si was highly significantly correlated with most of the elements (Si with Na = 0.73, Al = 0.81, Ca = 0.79, Fe = 0.86, Cu = 0.93, Zn = 0.72 and K = 0.61) suggesting common origin or occurrence. High correlation also corroborated the XRD study which shows the presence of silica in different minerals like wollastonite, vermiculite, kaolinite and quartz (SiO<sub>2</sub>) as shown in Figs. 3 and 4. Another highly significant correlation was observed for Ca (Ca with Na = 0.63, Al = 0.83, Si = 0.79, Fe = 0.76, Cu = 0.88, and Zn = 0.77) implying its common sources. Good correlations between these elements also suggest occurrence of calcium aluminum silicates, calcites and calcium iron oxides at the study site (Figs. 3 and 4). These particles mostly originated from construction, natural soil and vegetation burning (Shandilya and Kumar 2010). Positive correlation between transition elements like Fe and Zn (as Fe<sub>3</sub>Zn<sub>10</sub> in Fig. 3) was also observed (*r* = 0.82)

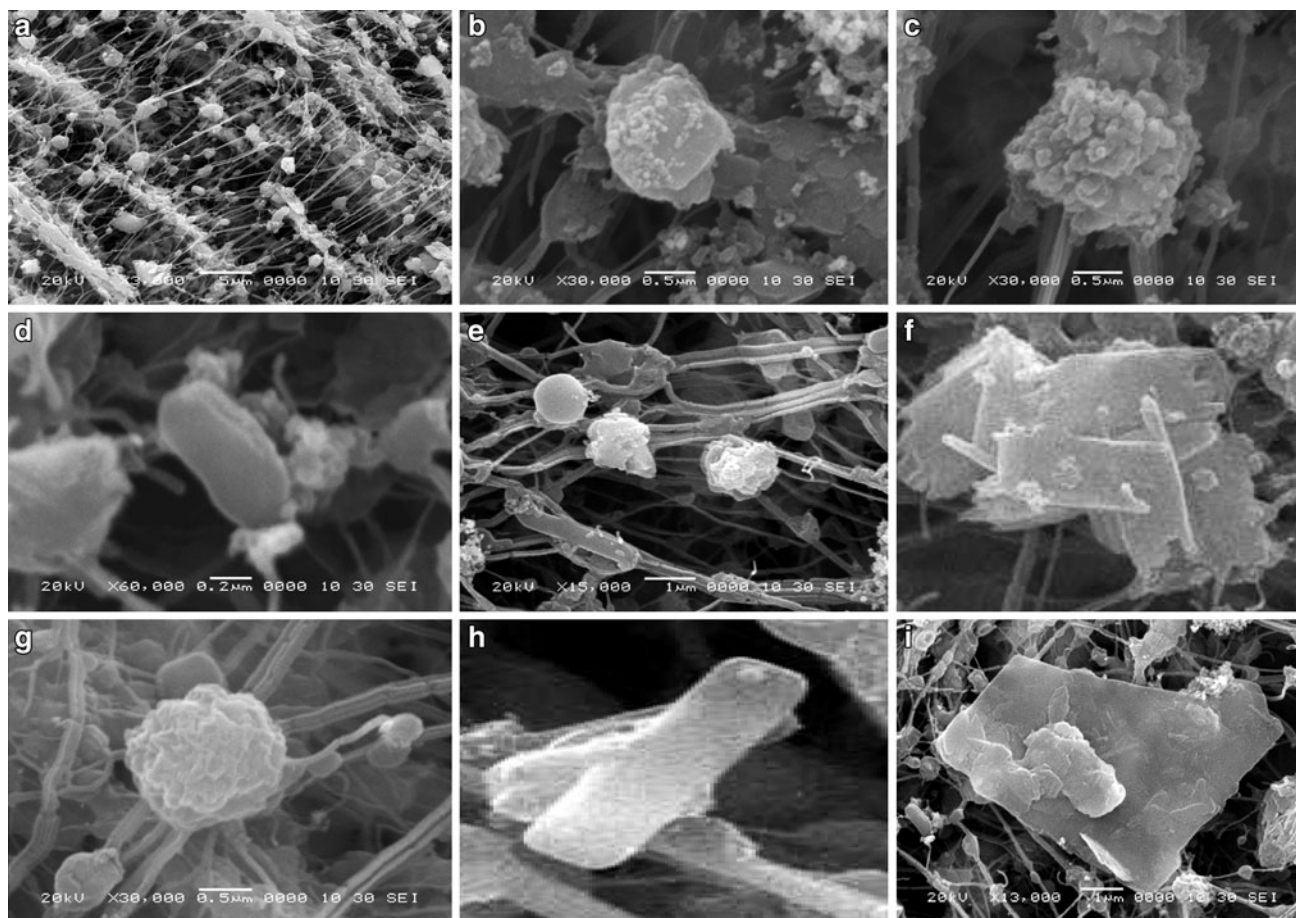


**Fig. 5** Micrographs of **a** different particles deposited on filter paper, **b** isolated crystal of halite along with soot particles (EDS: Na, Cl, S, C; size 1.25  $\mu\text{m}$ ), **c** soot particles (EDS: C, O, S), **d** capsule shape along with soot particles (EDS: S, Fe, Cu; size 0.34  $\mu\text{m}$ ), **e** smooth

surface (tar balls, EDS: C, Fe; size: 1.06  $\mu\text{m}$ ) and rough surfaces (size 1.2 and 1.37  $\mu\text{m}$ ), **f** twinned crystal aggregates of gypsum (EDS: Ca, S), **g** rough spherical (EDS: Si, Al, Ca, size: 1.47  $\mu\text{m}$ ), **h** rod shape (EDS: Ca, C, O), **i** aluminosilicate (EDS: Si, Al, O; size:  $\sim 5$   $\mu\text{m}$ )

**Table 2** Correlation coefficient of different elements in  $\text{PM}_{2.5}$  of study area

	C	O	Na	Al	Si	P	S	Ca	Mg	Fe	Cu	Zn	K
C	1												
O	-0.12	1											
Na	0.34	0.26	1										
Al	<b>0.84*</b>	-0.19	0.70	1									
Si	<b>0.69*</b>	-0.09	<b>0.73*</b>	<b>0.81**</b>	1								
P	0.43	<b>0.80**</b>	0.30	0.24	0.13	1							
S	-0.36	0.50	0.25	0.12	0.003	-0.65	1						
Ca	<b>0.79*</b>	-0.38	<b>0.63*</b>	<b>0.83**</b>	<b>0.79**</b>	0.03	0.20	1					
Mg	0.51	0.11	0.53	<b>0.66*</b>	0.24	0.48	0.13	0.57	1				
Fe	0.56	-0.46	0.34	0.66	<b>0.86**</b>	-0.19	-0.05	<b>0.76*</b>	-0.06	1			
Cu	<b>0.88**</b>	-0.04	0.22	<b>0.94**</b>	<b>0.93**</b>	0.35	-0.11	<b>0.88**</b>	0.53	<b>0.75*</b>	1		
Zn	<b>0.94**</b>	-0.34	0.22	0.77*	0.72*	0.17	-0.31	<b>0.77*</b>	0.25	<b>0.82*</b>	<b>0.83*</b>	1	
K	0.08	-0.52	0.52	0.53	<b>0.61*</b>	-0.59	0.57	0.59	-0.10	<b>0.69*</b>	0.42	0.27	1

\* Correlation is significant at the 0.05 level (2-tailed)

\*\* Correlation is significant at the 0.01 level (2-tailed)

**Table 3** Factor loading of the elements present in the study area

	Factor 1	Factor 2	Factor 3
C	<b>0.98</b>	0.20	0.06
O	0.01	<b>0.91</b>	−0.4
Na	<b>0.88</b>	0.14	0.12
Al	<b>0.99</b>	−0.12	0.06
Si	<b>0.84</b>	0.11	<b>0.53</b>
P	0.37	<b>0.78</b>	−0.50
S	0.14	<b>0.97</b>	0.18
Ca	<b>0.72</b>	<b>0.56</b>	0.23
Mg	0.16	<b>0.96</b>	0.15
Fe	<b>0.59</b>	−0.07	<b>0.80</b>
Cu	<b>0.56</b>	0.14	<b>0.84</b>
Zn	<b>0.59</b>	0.08	<b>0.73</b>
K	<b>0.52</b>	−0.47	<b>0.77</b>
Eigen value	5.2	2.9	2.5
% Variance	50.8	26.6	20.6
Attributed sources	Soil and building material	Oil combustion	Biomass burning

Factor loading above 0.5 are highlighted in bold

suggesting common source. *P* was highly correlated with O and Mg which was also observed by XRD analysis and is present in the Pune atmosphere as a mineral  $Mg_2P_4O_{12}$  (Fig. 3).

To determine the associations between elements which correspond to the main elements observed and generated by diverse emission sources, factor analysis was attempted on entire data set. Soot particles were not considered in the factor analysis therefore it has been discussed separately. Table 3 presents the loading of the main groups of particles present in Pune site (SPSS, ver. 16). On the basis of the factors acquired, morphology and composition of PM of that factor is discussed as under.

#### *Factor 1: soil and building material erosion*

Factor 1 represents 44.6 % of the total variance. This particular category consists of Na, Al, Si, Ca, Mg, K and Fe. This factor represents the silica (Si, Al, Ca), feldspar (Si, Al and K), silicates from building materials (Si, Al, Ca, Fe; Si, Ca, Fe; Si, Ca; Si, Fe, etc.) and Ca and Mg carbonates. These results were corroborated with the minerals analyzed by XRD (Figs. 3 and 4). Thus, first category belongs to soil and building material erosion.

$SiO_2$  and aluminosilicates are the main types of silicon-bearing particles observed in this study as analyzed from the XRD study (Figs. 3 and 4). They both can be assigned to natural and anthropogenic origin. Aluminosilicates with spherical shapes come from anthropogenic source and they could arise from combustion processes,

in contrast to irregularly shaped particles that are classified as natural (earth's crustal matter). Most of these are seen in agglomerated consisting of the smaller particles and enriched by the heavy metals as Fe, Cu and Zn. This type of PM mainly originated from the construction activities and industries. This is corroborated with the ongoing construction and industrial activities in the proximity of sampling site. In the present site, silicate particles such as quartz are part of natural origin. Figure 6a shows SEM of the irregular particle with the high percentage of Si, Al and O suggesting its origin from geological and building materials, which have undergone traffic-induced abrasion and re-suspension process. Figure 6b shows the smooth spherical particles along with its elemental mapping. This smooth particle could be fly ash. Fly ash is the byproduct of coal burning containing mostly aluminosilicates (Chang et al. 1999). Li and Shao (2009a) also suggest that particles contain Si, O and Al with minor Ca, Ti, Mn and Fe as spherical fly ash. In present study, elemental mapping also demonstrate that particles are highly enriched with Al, Si, Ca along with the Fe and Ti which implies that it is fly ash. In our study, silicates contribute ~52 % of the total minerals. Silicate can act as greenhouse particles due to the fact that the outgoing radiation is in the infrared and have absorption bands in this wavelength (Rodriguez et al. 2009). High percentage of silicate mineral definitely affects the climate of the city.

Calcium carbonates particles have also been frequently observed in airborne PM sample (Ro et al. 2001; Li et al. 2003). In this study, presence of calcite ( $CaCO_3$ ) and dolomite ( $Ca Mg (CO_3)_2$ ) have also been identified by XRD study (Fig. 3). These alkaline particles can absorb the acidic gases such as  $SO_2$  and  $NO_2$  (Li and Shao 2009b) and help to reduce the acidity of PM. Even though, percentage contribution of this mineral is relatively very low. SEM and EDS mapping results are shown in Fig. 7 where qualitative identification of the elemental composition of the particles of a selected area of the filter paper showed the distribution of the Ca, C and O along with some Si particles implies the presence of  $CaCO_3$ . The SEM micrograph in Fig. 7 showed that the particle on the filter paper tend to form large conglomerates of smaller Ca particles interspersed with the significant amounts of C and O. The elemental EDS scan also showed the amount of Si in very small particles. Presence of these minerals in Pune City may be due to the site, which is covered with the rocky hills.

The presence of halite in the PM of Pune can be explained by the proximity of the sea. Halite and other sea particles are important light scatterers and efficient condensation nuclei and they provide large surface area for atmospheric reactions.

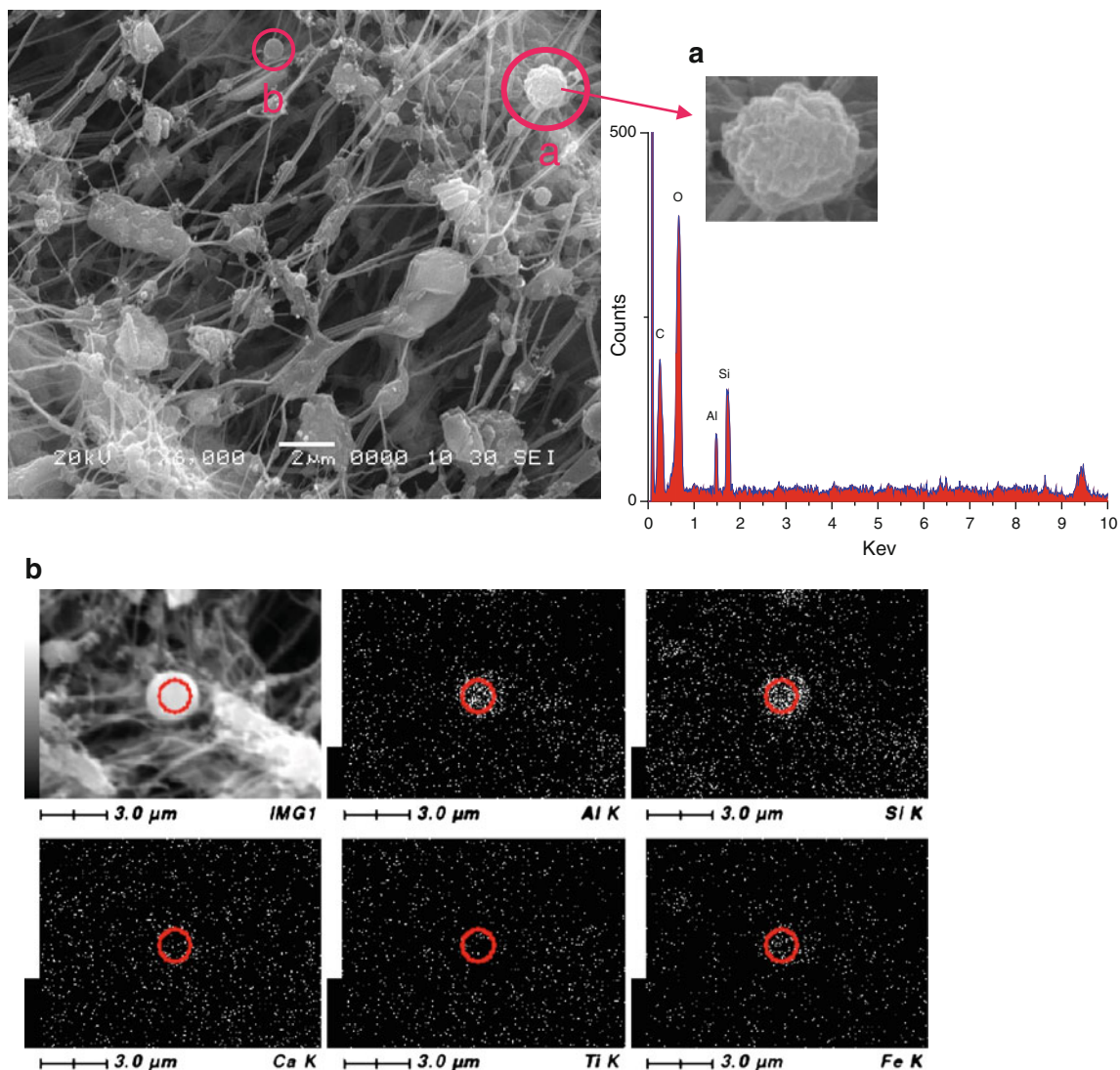


**Fig. 6** SEM–EDS image of **a** natural silicates and **b** anthropogenic silicate particles

### Factor 2: oil combustion

Factor 2 accounted for 20.6 % with high loading of S, P, Mg, and moderate loading of Ca. This group comes from the particles probably emitted by the combustion of the automobile oil. Anthropogenic released particles might have absorbed on the existing mineral shows congregation of these elements in this factor.

S-bearing particles are very common in ambient PMs. They are found in virtually all airborne PM samples (Buseck and Pósfai 1999; Pósfai et al. 2003). S is present in atmosphere in the form of sulfate. In the present study, sulfur concentrations were found to be  $615 \text{ ng m}^{-3}$  (unpublished ICP data). The majority of sulfate in the present site is formed from  $\text{SO}_2$  due to the combustion of fossil fuels and biomass burning.  $\text{SO}_2$  may be absorbed on the mineral particles and form the secondary minerals (Li

and Shao 2009b). Silicate minerals are abundantly present in Pune (as depicted in Fig. 8) which can act as surrogate for the sulfurization. However, the calcite or dolomite or Ca-rich particles can be of importance to absorb the acidic materials. These particles are predominately in the fine fraction and therefore round in shape. In recent years, sulfurization on the surface of particles has also been reported by Lu Senlin et al. (2006). Figure 8 shows the particles enriched with Ca and S. Sulfur cluster often with sharp edges are mainly composed of  $\text{CaSO}_4$  (gypsum). The formation of this mineral may arise from the heterogeneous oxidation of  $\text{SO}_2$  on the existing mineral particles surface in the atmosphere. The internal and external mixing/reaction result the aggregated particles of gypsum after the evaporation of drops (sharp edges of gypsum seen in the Fig. 8). Type of aggregation of these particles is important because it affects radiative properties of the aerosols and

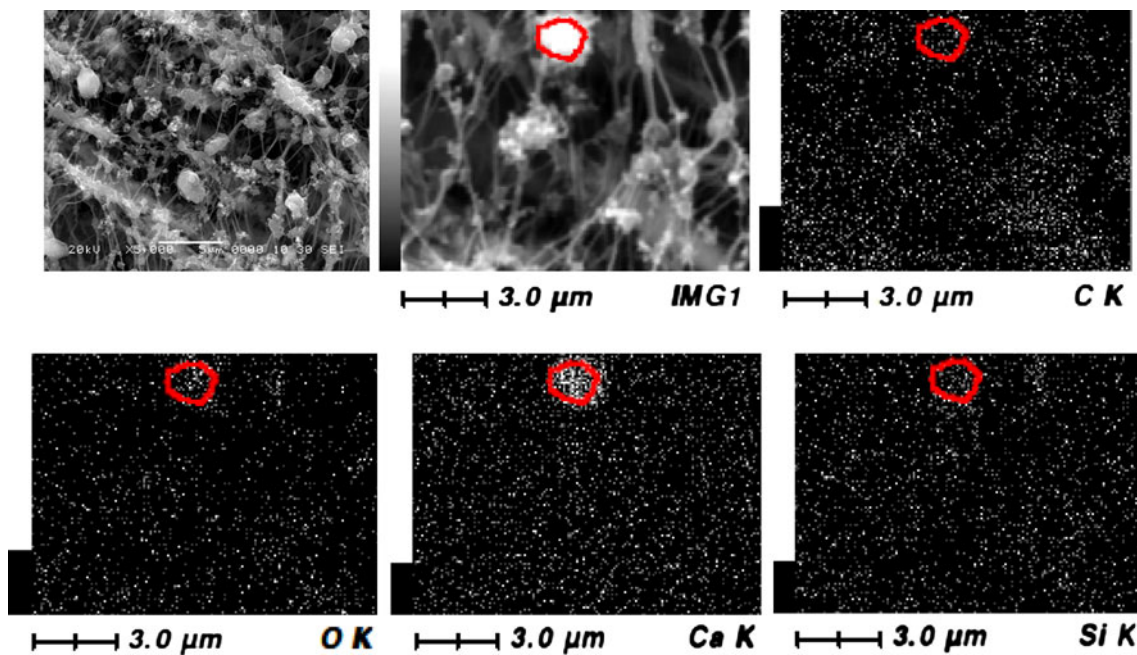


Fig. 7 SEM image of the particles and their elemental mapping exhibiting the CaCO<sub>3</sub> along with Si

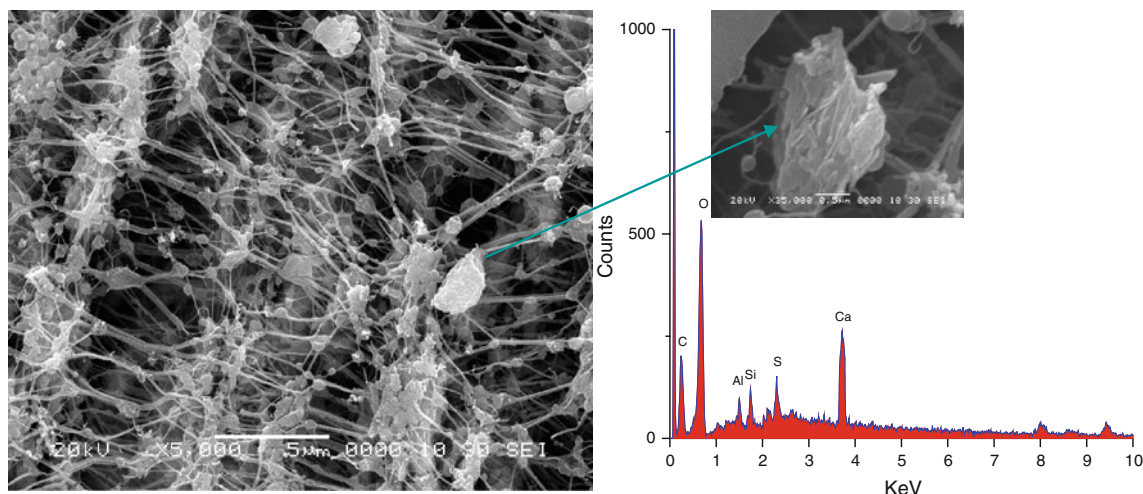


Fig. 8 SEM-EDS of sulfate particles

also it has the ability to act as cloud condensation nuclei (Rodriguez et al. 2009).

Other minor amount of mineral particles observed in this study includes phosphorus-bearing particles. These particles typically exist in the form of Mg<sub>2</sub>P<sub>2</sub>O<sub>7</sub> and SiP<sub>2</sub>O<sub>7</sub> (as shown in Fig. 3). Presence of SiP<sub>2</sub>O<sub>7</sub> mineral is shown in the Fig. 9. Mapping of these particles shows higher concentration of Mg, P and O which is present in Pune atmosphere. Concentration of P is also high in the analyzed samples (ICP results, unpublished data). Various organic phosphorus compounds have been used as combustion chamber deposit modifiers as well as corrosion inhibitor for motor gasoline and fuels. Thus, there is possibility that

automobile emission may contain toxic phosphorus compounds.

In the XRD study, kokaite and (NH<sub>4</sub>)<sub>2</sub>SO<sub>4</sub> have also been observed. It could be anthropogenic and formed by the reaction between NH<sub>4</sub>Cl and H<sub>2</sub>SO<sub>4</sub>. NH<sub>4</sub> is the main neutralizer of precipitation acidity. Presence of (NH<sub>4</sub>)<sub>2</sub>SO<sub>4</sub> in Pune atmosphere have already been reported by the other authors (Rao et al. 1992; Safai et al. 2005).

*Factor 3: fuel and biomass burning*

The third factor explaining the 18.3 % of total variance shows high loading of Fe, Cu, Zn, and K. This factor can be

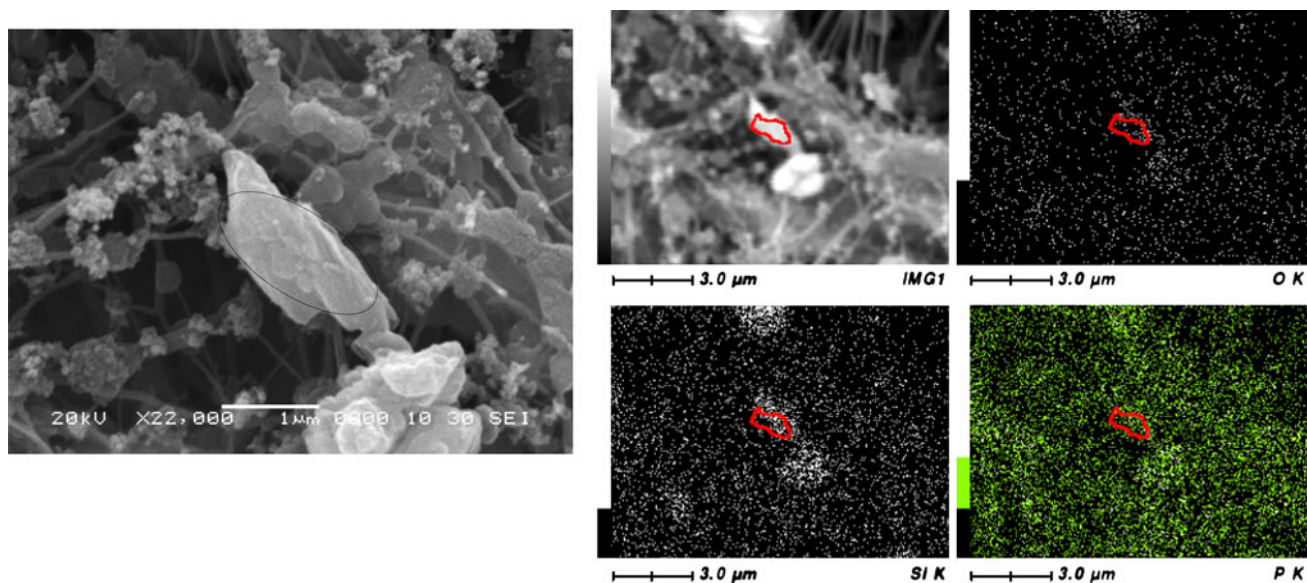


**Fig. 9** SEM image of particles and their elemental mapping ( $\text{SiP}_2\text{O}_7$ )

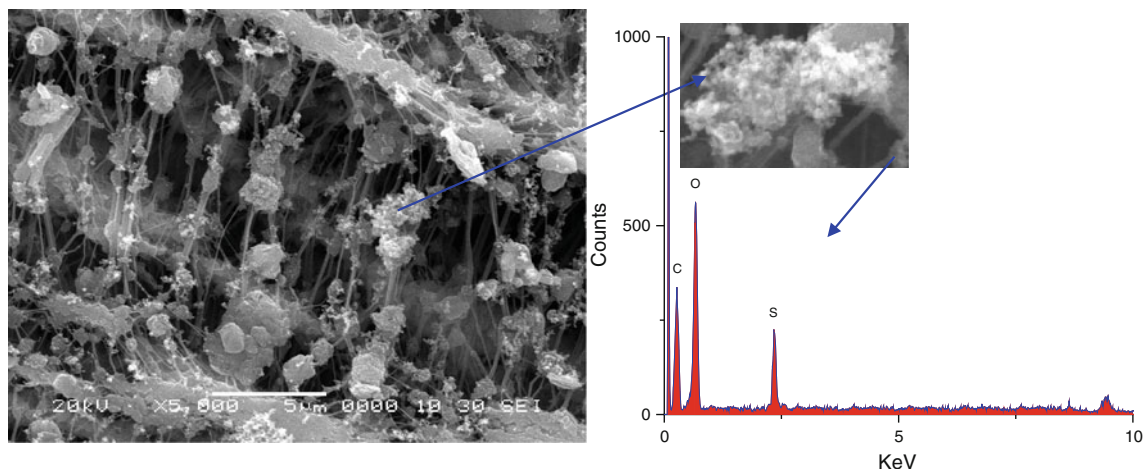


**Fig. 10** SEM-EDS of soot particle enriched with S

attributed to fuel (i.e., gasoline, natural gas and coal) and biomass burning. Cu and Zn could be released from wear and tear of vulcanized vehicle tires and corrosion of galvanized automobile parts as numerous old vehicles are plying on streets of Pune city. Adriano (2001) also reported that corrosion of the galvanized steel is a major source of Zn emission in the surface environment. K may be released into the atmosphere from vegetation and biomass burning as vegetation is one of the main sources of K (Penner 1995) in the University.

Furthermore, besides these three factors, soot particles are abundantly present in all studied samples. Present sampling site is about 1 km from the main traffic junction (University circle). In India, traffic congestion is the commonest problem. Traffic congestion leads to

incomplete combustion of fossil fuel, thus high concentration of soot particles are perceived in the micrograph (Fig. 10). Soot is present in agglomerates of many fine spherical particles with short chain structures (i.e., granulated) (Fig. 10). In general, soot morphology depends on the different types of fuels, burning condition and atmospheric processes (Yue et al. 2006). Soot particles are primarily emitted from burning and incomplete combustion of fossil fuels. Li et al. (2011) found the S-rich soot particles and suggested that soot particles from vehicular emissions underwent aging processes during transport. In the present study, C-rich particles are present in considerable percentage (by EDS data) along with the amount of S, mainly produced from the vehicular traffic as well as from the biomass burning. Aggregates of soot and S are

**Table 4** Comparison of morphological study of airborne particle and their respective origin

Area	Particle groups identified	Abundance	Morphology	Source	Origin	References
Mt. Qomolangma (Himalayas)	Soot/tar ball (C abundant, S minor)	8/3 %	Chain aggregation of carbonaceous spherules	Fuels, biomass burning, incomplete fossil fuel combustion	Natural and Anthropogenic	Cong et al. 2010
	Aluminosilicates	55 %	Irregular shape	Soil	Natural	
	Calcium sulfate	16 %	Irregular shape	Local crustal source	Natural + anthropogenic	
	Ca/Mg CO <sub>3</sub>	2 %	Irregular shape	Soil	Natural	
	Fe/Ti-rich particles	3 %	Irregular shape	Soil	Natural	
	Pb-rich particles	1 %	Spherules	Automobile, mining, waste incineration	Anthropogenic	
Portugal (background)	Biological particles	12 %	Variable morphology	Pollen, bacteria, excrements of insects	Natural	
	Aluminum silicates	63 %	–	Soil	Natural	Slezakova et al. 2008
	Fe oxides and alloys	18 %	–	Automobile and traffic	Traffic	
	Sulfates (Na & K)	15 %	–	Sea	Natural	
	Ti/Al rich	3 %/0.5 %	–	Soil	Natural	
Chandigarh, India	Lead sulfate	0.5 %	–	Traffic	Anthropogenic	
	Spherical fly ash	–	Spherical	–	Traffic	Sharma and Srinivas 2009
	Silica/aluminosilicates	–	Spherical and nonspherical	Crust	Natural + anthropogenic	
	Clay, quartz, calcite and gypsum	–	Irregular	Soil	Natural + anthropogenic	
	Cubical shaped salt particle	–	Cubic	Arabian sea	Natural	
Agra, India	Biological particles	–	Spherical and nonspherical	Grass pollens, corn smut	Natural	
	Aluminosilicates	2.2 %	Spherical and nonspherical	Crustal	Natural	Pipal et al. 2011
	Ca rich (CaCO <sub>3</sub> )	0.38 %	–	Construction, agriculture, natural soil	Natural + anthropogenic	
Pune, India	C-rich particles (soot and tar balls)	38.8 %	Flaky, chain and small aggregate of spherulite	Gasoline and coal burning	Anthropogenic	
	Aluminosilicates	52 %	Spherical irregular	Combustion process crustal (soil)	Anthropogenic natural	Present study
	Carbonates (CaCO <sub>3</sub> )	3 %	Irregular	Erosion of rocks	Natural	
	Halite (NaCl)	–	Cubic	Sea	Natural	
	Sulfate	8 %	Irregular	Biomass burning and fossil fuel	Anthropogenic	
	Soot	–	Agglomerates of fine particles, short chain	Burning and combustion of fossil fuel	Anthropogenic	

frequently observed in SEM analysis. This finding is also consistent with the Paoletti et al. (2003), who suggested that the S content on soot aggregate is probably the result from gas-to-particle conversion in the atmosphere. Such

particles are constituted of large number—hundreds of thousands of aggregates of carbonaceous microspherules having irregular morphology almost spherical to a long small chain (Paoletti et al. 2003; Li et al. 2011). In general,



soot particles are highly absorbing in nature and its presence in the atmosphere can change the sign of radiative forcing from negative to positive which leads to the heating of lower atmosphere (Menon et al. 2002; Tripathi et al. 2007), unlike most aerosols, which reflects light to space and have a global cooling effects.

#### Comparison of morphological study of airborne particles

Table 4 shows the comparison study of morphology of particles observed at various locations along with the present study. It is inferred from the Table 4, that aluminosilicate was the most abundant mineral [ $\sim 52$  to  $63$  % in all studies except in Agra ( $\sim 2.2$  %)] present with the irregular and spherical morphology. Irregular morphology of aluminosilicate has been reported at Mt. Qomolangma, Himalayas (Cong et al. 2010), and background site of Portugal (Slezakova et al. 2008) originated from natural sources as the sites are free from anthropogenic sources. While both irregular and spherical shaped aluminosilicates were observed at Agra (Pipal et al. 2011), Chandigarh (Sharma and Srinivas 2009) and Pune (present site) originated from natural as well as from anthropogenic sources. This is possibly due to the semi-urban/urban sites where mixture of the sources is predominantly present. Compared with aluminosilicate, the other minerals in PM collected from different locations showed variations, viz. Ca-rich particles with irregular morphology was found in all study samples from all locations but it could not be found in Portugal. It might be due to the negligible contribution of soil dust to airborne particles of background site of Portugal (Slezakova et al. 2008). Cubic shaped particles appeared only in the areas near coast such as in the present study (Pune) and in Portugal (Slezakova et al. 2008). Sulfate particles (i.e., gypsum) and  $\text{CaCO}_3$  with irregular shape have been observed at Mt. Qomolangma (Cong et al. 2010), Agra (Pipal et al. 2011) and in present study and originated from natural and anthropogenic sources. Besides that, C-rich particles (i.e., soot) have also been observed as agglomerates of fine particles and short chain in Pune (present study), Agra and Mt. Qomolangma (Table 4).

#### Conclusion

The SEM–EDS technique is a valuable tool for the characterization of PM especially for individual particles, whereas XRD technique is for identification of minerals. Additionally, the identification of the morphology and chemical composition of these particles provides valuable information for the determination of their origin and formation processes. The results presented in this paper show

the presence of diversity of particles from natural and anthropogenic origin. XRD study revealed that  $\text{PM}_{2.5}$  is mostly made up of silicates followed by oxides, sulfates, phosphates, carbonates and others. The factorial analysis of the results from SEM–EDS microanalysis determined the main elements of the different particles groups and related them to their origin. Factor 1 represents  $\sim 44.6$  % of the total variance and attributed to soil and building material erosion. In this factor, silicates are the major minerals which are both natural and anthropogenic (as fly ash) origin followed by carbonates (calcite and dolomite) are mainly natural origin as site is covered with hills. Factor 2 corresponds to oil combustion as the source with  $20.6$  % of total variance. In this factor, S, P and Mg along with moderate Ca are grouped together. S mainly originated from the burning of fuel and deposited on the existing minerals due to sulfurization process. This factor represents the secondary minerals like gypsum ( $\text{CaSO}_4$ ),  $\text{Mg}_2\text{P}_2\text{O}_7$  and  $\text{SiP}_2\text{O}_7$  as indicated by the XRD study also. The third factor explaining the  $18.3$  % of total variance shows high loading of Fe, Cu, Zn, and K. This factor can be attributed to fuel and biomass burning. Besides these, soot particles are abundantly present in all studied samples. Mineral particles as sulfates aggregated to soot could have produced localized climatic effect in Pune. The increase of the mean temperature and the precipitation in the city since past few years could be related to the high loading of PM. A more detailed characterization of individual particles and a better knowledge of the processes that lead to their formation are needed to obtain more conclusive results.

**Acknowledgments** Authors wish to thank Department of Science and Technology (DST No. SR/FTP/ES-91/2009), New Delhi and BCUD (BCUD/OSD/184 (Sr. No. 9), Pune, for financial assistance. Authors also express their gratitude to Head, Department of Chemistry, University of Pune, for his encouragement. Mr. Shinde and Mr. Jagtap, Department of Physics, University of Pune, are also acknowledged for analyzing the samples for SEM–EDS and XRD.

#### References

- Adachi K, Chung SH, Buseck PR (2010) Shapes of soot aerosol particles and implications for their effects on climate. *J Geophys Res* 115 (D15206), doi:10.1029/2009JD012868
- Adriano DC (2001) Trace elements in terrestrial environments—biogeochemistry, bioavailability and risks of metals, 2nd edn. Springer, New York
- Andreae MO (1995) Climatic effects of changing atmospheric aerosol levels. In: Henderson-Sellers A (ed) Future climates of the World: a modeling perspectives. World survey of climatology, vol 16, Elsevier, Amsterdam, p 341–392
- Berube KA, Jones TP, Housley DG, Richards RJ (2004) The respiratory toxicity of airborne volcanic ash from the Soufriere Hills volcano, Montserrat. *Mineralog Mag* 68(1):47–60
- Breed CA, Arocena JM, Sutherland D (2002) Possible sources of  $\text{PM}_{10}$  in Prince George (Canada) as revealed by morphology and

- in situ chemical composition of particulate. *Atmos Environ* 36:1721–1731
- Buseck PR, Pósfai M (1999) Airborne minerals and related aerosol particles: effects on climate and the environment. In: Proceedings of the National Academy of Sciences of the United States of America
- Buseck PR, Jacob DJ, Pósfai M, Li J, Anderson JR (2000) Minerals in the air: an environmental perspective. *Int Geol Rev* 7:577–594
- Chabas A, Lefevre RA (2000) Chemistry and microscopy of atmospheric particulates at Delos (Cyclades-Greece). *Atmos Environ* 34:225–238
- Chang H-L, Chun C-M, Aksay IA, Shih W-H (1999) Conversion of fly ash into mesoporous aluminosilicate. *Ind Eng Chem Res* 38:937–977
- Cong Z, Kang S, Dong S, Liu X, Qin D (2010) Elemental and individual particle analysis of atmospheric aerosols from high Himalayas. *Environ Monit Assess* 160:323–335
- Dentener FJ, Carmichael GR, Zhang Y, Lelieveld J, Crutzen PJ (1996) Role of mineral aerosol as a reactive surface in the global troposphere. *J Geophys Res* 101:22869–22889
- Dockery D, Pope C, Xu X, Spengler J, Ware J, Fay M, Ferris B, Speizer F (1993) An association between air pollution and mortality in six US cities. *N Engl J Med* 329:1753–1759
- Duce RA (1995) Source distributions and fluxes of mineral aerosols and their relationship to climate. In: Charlson RJ, Heintzenberg J (eds), *Aerosol forcing of climate*, Wiley, New York
- Ekosse G, van den Heever DJ, de Jager L, Totolo O (2004) Environmental chemistry and mineralogy of particulate air matter around Selebi Phikwe nickel–copper plant, Botswana. *Miner Eng* 17:349–353
- Ghio AJ, Devlin RB (2001) Inflammatory lung injury after bronchial instillation of air pollution particles. *Am J Respir Crit Care Med* 164:704–708
- Jung CH, Kim YP (2006) Numerical estimation of the effects of condensation and coagulation on visibility using the moment method. *J Aerosol Sci* 37(2):143–161
- Kunzly N, Kaiser R, Medina S, Studnicka M, Chanel O, Fillinger P, Herry M, Horak Jr F, Puybonnieux-Texier V, Quénel P, Schneider J, Seethaler R, Vergnaud J-C, Sommer H (2000) Public-health impact of outdoor and traffic-related air pollution: a European assessment. *Lancet* 356:795–801
- Li W, Shao L (2009a) Transmission electron microscopy study of aerosol particles from the brown hazes in northern China. *J Geophys Res* 114:D09302. doi:10.1029/2008jd011285
- Li W, Shao L (2009b) Observation of nitrate coatings on atmospheric mineral dust particles. *Atmos Chem Phys* 9:1863–1871
- Li XY, Gilmour PS, Donaldson K, MacNee W (1996) Free radical activity and pro-inflammatory effects of particulate air pollution (PM<sub>10</sub>) in vivo and in vitro. *Thorax* 51:1216–1222
- Li J, Pósfai M, Hobbs PV, Buseck PR (2003) Individual aerosol particles from biomass burning in southern Africa: 2. Compositions and aging of inorganic particles. *J Geophys Res-Atmos* 108, SAF 20/1–SAF 20/12
- Li W, Shao L, Shen R, Yang S, Wang Z, Tang U (2011) Internally mixed sea salt, soot and sulphate at Macao, a coastal city in south China. *J Air Waste Manage Assoc* 61(11):1166–1173
- Lu Senlin, Longyi S, Minghong Wu, Zheng J (2006) Mineralogical characterization of airborne individual particulates in Beijing PM<sub>10</sub>. *J Environ Sci* 18(1):90–95
- Liu X, Zhu J, Espen PV, Adams F, Xiao R, Dong S (2005) Single particle characterization of spring and summer aerosols in Beijing: formation of composite sulfate of calcium and potassium. *Atmos Environ* 39:6909–6018
- Ma CJ, Kasahara M, Holler R, Kamiya T (2001) Characteristics of single particles sampled in Japan during the Asian dust storm period. *Atmos Environ* 35:2707–2714
- Mathis U, Kaegi R, Mohr M, Zenobi R (2004) TEM analysis of volatile nanoparticles from particle trap equipped diesel and direct-injection spark-ignition vehicles. *Atmos Environ* 38:4347–4355
- Menon S, Hansen J, Nazarenko L, Luo Y (2002) Climate effects of black carbon aerosols in China and India. *Science* 297:2250–2253
- Paoletti L, De Berardis B, Arrizza L, Passacantando M, Inglessis M, Mosca M (2003) Seasonal effects on the physico-chemical characteristics of PM<sub>2.1</sub> in Rome: a study by SEM and XPS. *Atmos Environ* 37:4869–4879
- Penner JE (1995) Carbonaceous aerosol influencing atmospheric radiation: black carbon and organic carbon. In: Charlson RJ, Heintzenberg J (eds) *Aerosol forcing of climate*. Wiley, England, pp 91–108
- Pina AA, Villasenor GT, Fernandez MM, Kudra AL, Ramos RL (2000) Scanning electron microscope and statistical analysis of suspended heavy metal particles in San Luis Potosi, Mexico. *Atmos Environ* 34:4103–4112
- Pina AA, Villasenor GT, Jacinto PS, Fernandez MM (2002) Scanning and transmission electron microscope of suspended lead-rich particles in the air of San Luis Potosi, Mexico. *Atmos Environ* 36:5235–5243
- Pipal AS, Kulshrestha A, Taneja A (2011) Characterization and morphological analysis of airborne PM<sub>2.5</sub> and PM<sub>10</sub> in Agra located in north central India. *Atmos Environ* 45:3621–3630
- Pósfai M, Simonics R, Li J, Hobbs PV, Buseck PR (2003) Individual aerosol particles from biomass burning in southern Africa: 1. Compositions and size distributions of carbonaceous particles. *J Geophys Res-Atmos* 108, SAF 19/1–SAF 19/13
- Quality of Urban Air Review Group (QUARG) (1996) Airborne particulate matter in the United Kingdom: 3rd report. Department of the Environment, London, pp 1–176
- Querol X, Alastuey A, Lopez-Soler A, Mantilla E, Plana F (1999) Mineralogy of atmospheric particles around a large coal-fire power station. *Atmos Environ* 30:3557–3572
- Querol X, Alastuey A, de la Rosa J, Sanchez de la Campa A, Plana F, Ruiz CR (2002) Source apportionment analysis of atmospheric particulates in an industrialized urban site in southwestern Spain. *Atmos Environ* 36:3113–3125
- Rao PSP, Khemani LT, Momin GA, Safai PD, Pillari AG (1992) Measurements of wet and dry deposition at an urban location in India. *Atmos Environ* 26:73–78
- Ro CU, Oh K-Y, Kim H, Chun Y, Osa'n J, Hoog J, Van Grieken R (2001) Chemical speciation of individual atmospheric particles using low-Z electron probe X-ray microanalysis: characterizing “Asian dust” deposited with rainwater in Seoul, Korea. *Atmos Environ* 35:4995–5005
- Rodriguez I, Gali S, Marcos C (2009) Atmospheric inorganic aerosol of a non-industrial city in the centre of an industrial region of the North of Spain, and its possible influence on the climate on a regional scale. *Environ Geol* 56:1551–1561
- Safai PD, Rao PSP, Momin GA, Ali K, Chate DM, Praveen PS, Devera PCS (2005) Variation in the chemistry of aerosols in two different winter seasons at Pune and Sinhgad, India. *Aerosol Air Qual Res* 5(1):115–126
- Schwartz J, Dockery DW, Leas LM (1996) Is daily mortality associated specifically with fine particles? *J Air Waste Manage Assoc* 46:927–936
- Shandilya KK, Kumar A (2010) Morphology of single inhalable particles inside public transit biodiesel fueled bus. *J Environ Sci* 22(2):263–270
- Sharma S, Srinivas M (2009) Study of chemical composition and morphology of airborne particles in Chandigarh, India using EDXRF and SEM techniques. *Environ Monit Assess* 150:417–425



- Shi Z, Shao L, Jones TP, Whittaker AG, Lu S, Berube KA (2003) Characterization of airborne individual particles collected in an urban area, a satellite city and a clean air area in Beijing. *Atmos Environ* 37:4097–4108
- Slezakova K, Pires JCM, Pereira MC, Martins FG, Alvin-Ferraz MC (2008) Influence of traffic emissions on the composition of atmospheric particles of different sizes-Part 2: SEM EDS characterization. *J Atmos Chem* 60:221–236
- Srivastava A, Jain V, Srivastava A (2009) SEM–EDX analysis of various sizes aerosols in Delhi India. *Environ Monit Assess* 150:405–416
- Suzuki K (2006) Characterization of airborne particulates and associated trace metals deposited on tree bark by ICP-OES, ICP-MS, SEM–EDX and laser ablation ICP-MS. *Atmos Environ* 40:2626–2634
- Tripathi SN, Srivastava AK, Day S, Satheesh SK, Krishnamoorthy K (2007) The vertical profile of atmospheric heating rate of black carbon aerosols at Kanpur in northern India. *Atmos Environ* 41:6909–6915
- Wheeler AJ, Williams I, Beaumont RA, Hamilton RS (2000) Characterisation of particulate matter sampled during a study of children’s personal exposure to airborne particulate matter in a UK urban environment. *Environ Monit Assess* 65:69–77
- Wilson WE, Suh HH (1997) Fine particles and coarse particles: concentration relationships relevant to epidemiologic studies. *J Air Waste Manag Assoc* 47:1238–1249
- Xie RK, Seip HM, Liu L, Zhang DS (2009) Characterization of individual particles in Taiyuan city, China. *Air Qual Atmos Health* 2:123–131
- Yue W, Li X, Liu J, Li Y, Yu X, Deng B (2006) Characterization of PM<sub>2.5</sub> in the ambient of Shanghai city by analyzing individual particles. *Sci Total Environ* 368(2–3):916–925
- Zhang Y, Carmichael GR (1999) The role of mineral aerosol in tropospheric chemistry in East Asia—a model study. *J Appl Meteorol* 38:353–366
- Zhu Y, Hinds WC, Seongheon K, Shen S, Sioutas C (2002) Study of ultrafine particles near a major highway with heavy-duty diesel traffic. *Atmos Environ* 36:4323–4335

